Evaluating Nitrogen Utilization Strategies in *Chlamydomonas reinhardtii*

Miku Tibule, 7915977

Advisor: Dr. Jae-Hyeok Lee

A thesis submitted to the Department of Biological Sciences, University of Manitoba,

in partial fulfilment of the requirements for the course

BIOL 4100 (Honours Thesis)

for the degree of

Bachelor of Science (Honours)

Abstract

Nitrogen (N) is a common, yet essential macronutrient required for nucleic acid and amino acid synthesis for cell growth and biomass of photosynthetic eukaryotes which includes algae and plants. Understanding how organisms strategically use N for growth will allow development of economical use of N fertilizer being invested into croplands, which in return mitigates anthropogenic contribution to environmental pollution. This honours thesis explores N-use strategies by examining the N-sensing mechanisms within *Chlamydomonas reinhardtii* to investigate its necessity for optimal growth under N-limited and N-repleted conditions through comparative growth within individual N source provision of NH_4Cl, KNO_3, and urea. Using photobioreactor and nitrogen quantification experiments, I obtained biomass productivity data and residual N within the cultures, which allowed for an understanding of algal growth under various N-source concentration conditions. Through a comprehensive data analysis of growth biomass OD and residual N concentrations, my study uncovered that there is a regulatory mechanism of *C. reinhardtii* that allows for a reduction in N consumption rate under extreme N limitation stress, which in turn allows the algae to shift its metabolic priorities to internal N-use. These insights contribute to the existing literature by highlighting the significance of the N-sensing mechanism within *C. reinhardtii,* for N-use strategies, discovering a temporal switch in metabolic function, and offering potential further investigations into how the algae prioritize cellular N contents for growth and cellular division. Ultimately, this study provides a deeper understanding of N assimilation and cellular use, paving the way for future research and developments in the field.

Acknowledgements

Thank you to Dr. Jae-Hyeok Lee for supervising me throughout my Honour's Thesis project, and to Dr. John Markham and Jennifer Doering for being a part of my Honour's Thesis committee and providing feedback on my work throughout the project. I would also like to thank Oyinkansola Oyateru for volunteering to assist me with certain tasks that contributed to my experiments.

Table of Contents

List of Figures

List of Tables

1 – Introduction

1.1 Understanding Nitrogen Use Efficiency

The United Nations (2019) has projected that the human population will rise to 9.7 billion by 2050. Increasing agricultural productivity and securing food products in unstable environments where arable land has decreased due to anthropogenic causes that result in droughts, floods, and rapidly changing climate conditions is the current challenge that the world faces (Kant et al., 2011). At the beginning of the 1960s population boom, agricultural industries began the eutrophication of arable land by using synthetic N fertilizers to increase crop yield abundance while simultaneously transforming nature reserves for more farmland. (Tilman et al., 2001; Firbank 2005). The idea was to take advantage of the crops' N use efficiency (NUE) defined by the obtainable yield per available N unit in the soil (Hirel et al., 2011). From 1961 to 2006, synthetic N fertilizer use started from 11.6 million tonnes (Tg) to 104 Tg, increasing by 7.4-fold, but the total crop yield sought an increase of only 2.4-fold (Hirel et al., 2011). As crops can only use about 30% of the applied N within the soil, much of the applied N in the fields is lost in soil leaching and run-offs (Tilman et al., 2002; Hirel et al., 2011; Kant et al., 2011). With the increasing global food demand and N fertilizer overuse contributing to climate change, sustainable agricultural strategies must be implemented, such as developing crops with higher NUE, to enhance agricultural productivity and mitigate anthropogenic effects on the environment (Kant et al., 2011; Fukase and Martin, 2020). Doing so requires taking advantage of photosynthetic eukaryotes' internal biological regulatory mechanisms involved in N assimilation strategies.

1.2 Nitrogen assimilation by photosynthetic eukaryotes

Nitrogen is an essential, rate-limiting macronutrient required for nucleic acid and amino acid synthesis for growth and survival of all living organisms including photosynthetic eukaryotes (Ota et al., 2020; Xu et al., 2012). Plants and algae can absorb N from the soil in inorganic N forms: ammonium (NH_4^+), nitrate (NO_3^-), and nitrite (NO_2^-); and organic N forms: urea, and amino acids (Saroussi et al., 2017). Of the two, inorganic N sources are more frequently assimilated by photosynthetic eukaryotes as they are more available within the environment, however, at high amounts, they incur toxic effects that limit the organism's growth and productivity (Giordano and Reven, 2014; Sanz-Luque et al., 2015). When N sources are assimilated into the cells, they are further processed into the glutamate synthase/glutamine-2-oxoglutarate aminotransferase (GS/GOGAT) cycle within the chloroplast, which relies on intracellular carbon (C) and N source availability to produce amino acids (Magasanik and Kaiser 2002; Fan et al., 2017; Rani et al. 2024).

Typically, NO_3^- and NH_4^+ are the major N sources taken by any photosynthetic eukaryotes based on their ability to be rapidly absorbed into the cytosol and sustained assimilation into the chloroplast with the support of the photosynthetic C supply (Fernandez and Galvan, 2007; Rani et al., 2024). NH_4^+ is considered preferred due to its energetically cost-effective assimilation compared to the NO_3^- assimilation (Liu and von Wirén, 2017). When NH_4^+ is absorbed into the cell through NH_4^+ transporters, it is rapidly transported into the chloroplast for the GS/GOGAT cycle (Liu and von Wirén, 2017; Rani et al., 2024). NO_3^- assimilation requires its expensive reduction into NH_4^+ for assimilation into the GS/GOGAT cycle (Liu and von Wirén, 2017; Rani et al., 2024).

NO_3^- is acquired through NO_3^-transporters and reduced to NO_2^- by cytosolic nitrate reductase (Guerrero et al., 1981; Fernandez and Galvan, 2007; Rani et al., 2024). NO_2^- is subsequently imported into the chloroplast by nitrate transporters to be further reduced to NH_4^+ by nitrite reductase (Fernandez and Galvan, 2007; Li et al., 2017; Rani et al., 2024). This process of reducing NO_3^- to NH_4^+ demands eight moles of electrons per mole of NO_3^-, consuming up to one third of high-energy electrons produced from photosynthesis during optimal growth (Hachiya & Sakakibara, 2016). Additionally, urea is another N source consumable by photosynthetic eukaryotes that also requires conversion into NH_4^+ for assimilation (Park et al., 2015; Tuttle et al., 2020; Liang et al., 2024). Different urea conversion systems exist across photosynthetic eukaryotes. For instance, plants, fungi, and bacteria can use urease systems. Algae can also use urease but could also have urea amidolyase complex with urea carboxylase and allophanate hydrolase subunits that they can utilize (Park et al., 2015; Liang et al., 2024).

Despite the high cost of assimilation, NO_3^- is one of the primary N sources used by photosynthetic organisms (Xu et al., 2012; Li et al., 2017; Rani et al., 2024). Under NO_3^--rich conditions, NO_3^- can be transported into cellular vacuoles for storage in plants (Wang et al., 2012; Fan et al., 2017). Conversely, most organisms cannot store NH_4^+ as its accumulation acidifies cells, and therefore, NH4+ is either turned straight into glutamine/glutamate or becomes released when extra (Hachiya & Sakakibara, 2016). This brings the question; what makes a better N source? Would organisms prefer assimilation efficiency or N capacity for N uptake? How would organisms respond if many N sources were presented together? How can we make use of those N-use strategies for engineering the improved N-use efficiency of the crop plants?

1.3 Responses to Nitrogen Limitation

Considering the dynamic availability of N source in nature, N sensing and regulation mechanisms become an integral component for organisms to supply necessary N sources for continuously fueling the GS/GOGAT cycle, especially under N-limited events. To cope with the N limitations in the environment, photosynthetic eukaryotes have developed N scavenging and N salvaging strategies for survival (Schmollinger et al., 2014; Saroussi et al., 2017; Munz et al., 2020). In N scavenging response, organisms upregulate genes required for the uptake and assimilation of N sources (Saroussi et al., 2017). When the alternative N-sources are still insufficient, the organism would then switch to N salvaging response which involves recycling internal N reservoirs through the degradation of chloroplast protein components, redundant ribosomes, and extra nucleic acids (Schmollinger et al., 2014; Saroussi et al., 2017; West, 2023). Differentiating these stepwise N-starvation responses from complete N-starvation is still a huge challenge when studying N-starvation signalling (Munz et al., 2020). For example, *Arabidopsis thaliana* (L.) Heynh has over 40 distinct cell types that continuously exchange N between source and sink tissues, forming a complex network of N-replete and N-limited cells (Munz et al., 2020).

In a study done with arginine-fed cultures of *Chlamydomonas reinhardtii* P.A.Dang, Munz et al. (2020) reported that these cultures reactivated N starvation marker genes and accumulated neutral lipids during normal exponential growth. This highlights the N scavenging response in which there is an imbalance in internal N to C supply—with less N, excess C is stored in forms either as starch or triacylglycerols (Schmollinger et al., 2014; Munz et al., 2020). This N scavenging response was tested with a mutant

strain that could not properly assimilate arginine involving its conversion into NH_4^+ outside of the cell (Munz et al., 2020; Jia et al., 2022). Additionally, Jia et al., (2022) observed that N scavenging genes were upregulated when *C. reinhardtii* cultures experienced a condition shift from 8.0 - 2.0 mM NH_4^+, despite not being starved of N. This could suggest that cellular N conditions involving external NH_4^+ trigger responses to N-limitation that are essential for N source assimilation.

1.4 Using *Chlamydomonas reinhardtii* as a Model Organism

Chlamydomonas reinhardtii is a unicellular green alga that has a simple, haploid genome which can be easily manipulated with genetic and molecular tools to allow immediate expressions of loss-of-function mutations for observable phenotypes (Harris, 2009; Kou, 2013; Salomé and Merchant, 2019; Zhang et al., 2019). This alga shares many genetic similarities to higher plants regarding their N assimilation pathways, allowing N studies in this organism to apply to higher crop plants (Fernandez and Galvan, 2007; Bellido-Pedraza et al., 2020). In previous studies, physiological responses of *C. reinhardtii* under N limitation stresses have been well-documented (Schmollinger et al., 2014; Saroussi et al., 2017; Munz et al., 2020; Jia et al., 2022). Aside from the mentioned N scavenging and N salvaging responses to N limitation, *C. reinhardtii* can also respond with gametogenesis— the transition into the sexual state to produce zygospores for survival under prolonged nutrient starvation (Salomé and Merchant, 2019). These responses allow for reliable identification of N conditions that activate a full spectrum of N starvation marker genes (Munz et al., 2020).

With *C. reinhardtii*, I tested the hypothesis of whether N-sensing mechanisms are necessary for optimal growth under N-limited and N-repleted conditions to find the N

source with the best nitrogen use efficiency (NUE) by assessing their uptake strategies and how they use N sources under N limitation. This thesis aims to determine how the N sensing program is integrated for observed N use strategies through biomass productivity measurements. Understanding this program will guide strategies to engineer improvement in NUE in plant crops. To test this objective, the growth of wild-type (WT) strains of *C. reinhardtii* was tested under NH_4Cl, KNO_3, and urea at different concentration conditions to obtain growth physiology activity.

2 – Materials and Methods

2.1 Strains and culture media

Chlamydomonas reinhardtii WT strains, CC5119 and CC5370, are maintained in the Lee Lab at University of Manitoba. Genotypes of the strains were confirmed in-house in the Lee Lab using genomic PCR before use. All strains were maintained in the mixotrophic medium tris-acetate-phosphate agar plate (TAP) which contains 8.0 mM ammonium chloride (NH_4Cl) and a pH of 7.0 ± 0.02. (Gorman and Levine, 1965). Unless otherwise stated, strains are cultured under low light at 30 μmol $m^{-2}s^{-1}$ and a temperature of 23°C (Harris, 2009).

N source conditions tested were ammonium chloride (NH_4Cl), potassium nitrate (KNO_3), and urea. These N sources were applied in nitrogen-free TAP (NF-TAP) liquid medium used in bioreactor experiments. All media were autoclaved at 121 °C for 66 min and pH balanced at 7.0 ± 0.02 (Gorman and Levine, 1965), except for urea which was added into the sterile NF-TAP liquid medium through a sterile 0.2 μm filter to prevent urea heat breakdown into NH_3.

2.2 Bioreactor

Parallel screening culture experiments were done in a small-scale photobioreactor instrument (Photon Systems Instruments (PSI) Multi-Cultivator MC 1000-OD) to cultivate algae in suspension with a maximum volume of 80.0 mL. The bioreactor allows for precise control of the cultures' environment. LED light intensity was set at 100 uE with a light-dark cycle alternating every 20 seconds. Temperature control was set at 23 °C, and biomass optical density (OD) measurement at 680 nm. Algal strains were harvested under sterile conditions in the laminar flow using an inoculation loop. Cells were resuspended for a minimum of 2 hours in NF-TAP aliquots to observe active N-starvation responses. Resuspension was required to ensure cells were not clumped and could equally react to the medium. A manual cell counting procedure was performed for cell inoculation. Each experiment had replicates and was duplicated to ensure confidence in result accuracy. Vessels were also randomized in the bioreactor slots to control any lurking variables, such as possible small systematic errors in any of the sensors. Systemic errors, such as background noise or incorrect OD start baseline measurements, were manually fixed by removing sudden OD value spikes to create a smooth growth curve. In rare occasions when OD measuring sensors malfunctioned, experiments were redone for triplicate values. The experiments ran until the cultures reached their maximum biomass growth, indicated by a plateau in the OD reading after several days.

2.3 Cell Counting

Before and after experiments, the cell number of the strains were evaluated using a haemocytometer (Bright-Line) under light microscopy (Axiostar plus) with cell fixation using glutaraldehyde (final 2%). Glutaraldehyde binds to most abundant nucleophiles of

amino groups and to sulfhydryl groups which leads to cell protein crosslinking that causes cell fixation (Griffiths, 1993; Kawahara et al., 1997). Cell counting before bioreactor experiments is used for inoculation calculations into the vessels, and for evaluating each culture every harvest at its lag, mid-log and stationary phases. Samples (1mL) from each culture are harvested at those critical growth periods to measure residual N source quantities.

2.4 Ammonium Quantification

Quantifying NH_4Cl as the N source of the cultures was done using a multiparameter photometer (Hanna Instruments HI83325) with the ammonia medium-range protocol. This protocol was adapted from the D1426 Nessler Method from the American Society for Testing and Materials' Manual of Water and Environmental Technology. Samples are harvested at volumes 0.5 mL or 1.0 mL, to fit within the confidence range, and diluted with NF-TAP to a total volume of 10.0 mL. The dilution mixture was then reacted with 200 uL of each Nessler reagents sodium hydroxide and potassium tetraiodomercurate (II) then measured for absorbance performed at 420 nm wavelength. Obtained OD values were recorded and plotted against experimental-made standard curves, made using the same protocol, to estimate remaining culture NH_4Cl concentrations.

2.5 Nitrate Quantification

These NO_3^- quantification methods were adapted and modified from Cawse (1967). For high-range nitration concentrations above 4.0 mM, 200 µL culture samples of KNO_3 bioreactor experiments were mixed with 1.60 mL of 5% perchloric acid. From this mixture, 1.0 mL was collected and measured in the NanoDrop One UV-Vis

Spectrophotometer instrument Thermo Fisher Scientific to obtain OD values at 230 nm. Samples between 4.0 mM – 1.0 mM, nitrate quantitation were done with 900uL 5% perchloric acid + 100uL KNO3 sample at 210 nm. For samples between 0.5 – 0 mM, Nitrate Quantitation was 900uL KNO3 sample + 100uL 5% perchloric acid at 220 nm. Three standard curves were made for each method to estimate the KNO_3 concentration in the culture.

2.6 Urea Quantification

Urea quantification protocol was adapted and modified from Chaney and Marbach (1962). For the higher-range urea culture samples between 4.0 and 1.0 mM, 100 µL of the samples were mixed with 950 µL of 50 mM phosphate buffer at 7.0 pH and 50 µL urease from *Canavalia ensiformis* (jack bean). Phosphate buffer is a competitive inhibitor of urease however, its inhibitory action decreases as pH increases from urease conversion of urea into ammonium (Krajewska and Zaborska, 1999). The urea-urease-phosphate buffer mixture was incubated for 30 minutes. Afterwards, 250 µL of the mixture was then reacted with 5 µL each of Nessler reagents sodium hydroxide and potassium tetraiodomercurate (II). For 1.0 – 0.5 mM urea culture samples, the urea-urease-phosphate buffer mixture contained 900 uL urea sample, 50 uL 1M Phosphate Buffer at 7.0 pH, 50 uL urease. These samples were incubated and reacted similarly to the higher-range urea samples. All samples were placed in a 96-well plate for measurement in a plate reader (BioTek Synergy H1 Microplate Reader) at 400 nm. This method required two standard curves to estimate urea concentrations in the culture.

2.7 Data Analysis

Data obtained from the bioreactors were extracted as .csv files and were imported into Microsoft Excel to highlight and remove any OD measurement noises within the data. Through this software, the lag phase was also trimmed out of the final growth curves produced in this study to focus on the start of the growth of the cultures. Afterwards, growth rate data was calculated within the first 10 hours of growth by using the formula:

$$\text{Growth Rate} = \frac{\text{OD}_{10\,\text{h}} - \text{OD}_{0\,\text{h}}}{10}$$

The doubling time was also calculated by taking the natural logarithm of the growth rate within 10 hours. One-way ANOVA statistical tests, performed in Microsoft Excel, was used for most of this study to identify the differences within the groups that were affected by an independent variable. This allows for identifying the significant differences between the cultures grown in various concentration conditions and how they compare to each other by biomass OD values, growth rate, doubling time, and cell density.

3 – Results

3.1 – NH_4Cl as an N Source

Chlamydomonas reinhardtii WT strains CC5370 (Fig. 1) and CC5119 (Fig. 2) were tested in separate photobioreactors. To confirm that these strains do behave normally, statistical analysis was performed using one-way ANOVA to compare their growth maximum and growth rate, and the doubling time in each NH_4Cl concentration condition using the data from Tables 1 and 2. The p-values and the compared F-statistical values to the F-critical values are 0.86; 0.022 < 5.32, 0.31; 1.15 < 5.32, 0.62; 0.26 < 5.32 for growth maximum, growth rate, and doubling time respectively. As all the p-values are greater than $\alpha = 0.05$ and F-statistical values are less than the F-critical values, there is no significant difference in physiological growth responses between CC5370 and CC5119. As they present similar responses under N limitation, the following photobioreactor experiments were run with these WT strains acting as each other's replicates. Additionally, comparing the concentration conditions was done using triplicate averages from both WT strain cultures.

In both Figures 1 and 2, there is a difference in growth maximum values between each NH_4Cl condition, except for 8.0 mM and 4.0 mM NH_4Cl conditions. One-way ANOVA test on growth OD values at mid-log and stationary phases from Table 3 of 8.0 mM and 4.0 mM NH_4Cl conditions showed no significant difference as p-value = 0.0003, F-statistical value = 2935.7 > F-critical value = 18.5. This shows that the WT strains can grow to their maximum biomass at a minimum of 4.0 mM NH_4Cl. Therefore, it is expected that, at the stationary phase, 8.0 mM NH_4Cl cultures should present with excess NH_4Cl than the rest of the cultures if cultures only require a minimum of 4.0 mM NH_4Cl.

To investigate this, I quantified the NH_4Cl concentrations within the medium. Quantifying the NH_4Cl concentrations at the critical growth phases required two standard curves. The standard curve in Figure 3A was used for 8.0 – 4.0 mM NH_4Cl culture samples requiring 1.0 mL volume to measure lower N concentrations, especially toward the end of the culture growth. Meanwhile, the standard curve in Figure 3B was used for culture samples requiring 0.5 mL volume to measure 4.0 – 0.5 mM NH_4Cl culture samples. The linear equation of the standard curves was used to convert absorbance values obtained during the NH_4Cl quantification protocol into concentration values. Quantification data of NH_4Cl concentration is presented in Table 3. At the mid-log phase, cultures grown at 4.0 mM – 0.5 mM have nearly expended all NH_4Cl in the medium but did not completely consume it, as 0.329 – 0.156 mM NH_4Cl remained in the medium. This was to be expected as previous literature has described that photosynthetic organisms have increased ability in NH_4^+ uptake and assimilation under N stress (Glibert et al., 2016). However, for 8.0 mM cultures at their mid-log phase, there was an excess of 3.0 mM NH_4Cl in the medium. As expected, 4.0 mM NH_4Cl is the threshold at which *C. reinhardtii* experiences N-limitation stress and begins to activate N-limitation responses. However, by the stationary phase, cultures continued to consume the NH_4Cl in the medium. The 8.0 mM cultures used the majority of the NH_4Cl within the medium, and the 4.0 mM – 0.5 mM consumed a fraction of the NH_4Cl that remained from the mid-log phase. Interestingly, all cultures did not completely consume the NH_4Cl at the stationary phase, with the 8.0 mM – 0.5 mM cultures having nearly 0.156 – 0.110 mM NH_4Cl remaining in the medium. This showed that once *C. reinhardtii* experienced N-stress

limitation, they began to reduce the consumption rate of NH_4Cl but prevented the complete consumption of N in their environment.

Regardless of the reduced consumption rate, *C. reinhardtii* cultures were still capable of growth. For 4.0 – 0.5 mM cultures, the reduction in consumption rates started at the mid-log phase and presented with growth OD values ranging from 1.11 ± 0.045 to 0.359 ± 0.036. Their growth OD values then grew between a range of 2.176 ± 0.068 and 0.528 ± 0.030 at the stationary phase. The cell density of the cultures also increased greatly between the mid-log and stationary phases, as seen in Figure 4. Using a one-way ANOVA, a significant difference was confirmed between cell density (p-value = 0.21; 2.0 < 6.0) and growth maximum (p-value = 0.18; 2.3 < 6.0) between the two phases, as seen with the provided p-value and F-test respectively. *C. reinhardtii*'s growth between the mid-log phase and stationary phase despite a reduced NH_4Cl consumption rate showed a possible regulatory mechanism that allowed the algae to switch N metabolic functions for biomass growth from N uptake to possible internal N use. This was also investigated with KNO_3 cultures.

3.2 – KNO_3 as an N source

Both WT strains CC5370 and 5119 acted as each other's replicates for these experiments as stated from the previous section. Like the NH_4Cl cultures, WT strains grown in the KNO_3 medium reached their maximum growth values at a minimum of 4.0 mM KNO_3 and began to show a decreasing pattern at lower concentrations of 2.0 – 0.5 mM (Fig. 5). To determine if there were any differences in N-limitation responses between NH_4Cl and KNO_3, culture evaluation values starting from 8.0 mM to 0.5 mM of both conditions were tested using one-way ANOVA. This test showed that there were no

significant differences between the growth maximum values (p-value = 0.87; F-stat. 0.03 < F-crit. 5.32), growth rate (p-value = 0.89; F-stat. 0.02 < F-crit. 5.32), doubling time (p-value = 0.20; F-stat. 1.95 < F-crit. 5.32). However, there was a significant difference in their cell density measured at the stationary phase (p-value = 0.04; F-stat. 5.69 > F-crit. 5.32). Comparing the cell density values of NH_4Cl (Table 3) and KNO_3 (Table 5), the cell density of KNO_3 cultures at the stationary phase is lower compared to NH_4Cl cultures despite having no significant difference in growth maximum values. This could be due to the KNO_3 cultures expending more energy towards the energetically costly assimilation of NO_3^-. Because of that, we could expect KNO_3 cultures to have more reserved N in the medium.

To determine the residual KNO_3^- in the culture medium, quantification of KNO_3 is performed in culture samples using standard curves in Figures 6A-C. The standard curve in Figure 6A was used for 32.0 – 4.0 mM KNO_3 culture samples. Figure 3B standard curve was used for 4.0 – 1.0 mM KNO_3 culture samples and Figure 3C was for 1.0 – 0.5 mM samples. The linear equation of the standard curves was used to convert absorbance values obtained during the KNO_3 quantification protocol into concentration values (Table 5). As expected, cultures grown in higher KNO_3 concentrations above 4.0 mM had reserved N remaining in the medium in the mid-log and stationary phases. Interestingly, by the mid-log phase, 1.0 mM and 0.5 mM had consumed most of the KNO_3 in their medium, whereas cultures grown in 2.0 mM and above had some reserves. Compared to the NH_4Cl, even 4.0 mM cultures had consumed most of the N in the medium at the mid-log phase. This shows that NO_3^- consumption is slower compared to NH_4^+. By the stationary phase, cultures grown in 4.0 – 0.5 mM had nearly consumed the entire KNO_3 in

their medium but not completely, like the NH_4Cl cultures, which showed reduced N consumption rates when N is nearly expended. However, there was some residual KNO_3 left in the medium in the 32.0 – 8.0 mM cultures. NH_4Cl cultures grown in 8.0 mM cultures had 0.156 ± 0.012 mM residual N while KNO_3 cultures had 3.87 ± 0.32 mM residual N. This shows slower consumption of KNO_3 compared to NH_4Cl

Regardless, growth of the cultures in 4.0 – 0.5 mM KNO_3 can still be observed between the mid-log phase and stationary phase despite the lower consumption rates. With a one-way ANOVA, a significant difference in cell density (p-value = 0.15; F-stat vs. F-crit: 2.8 < 6.0) and biomass OD (p-value = 0.17; F-stat vs. F-crit: 2.5 < 6.0) values between the mid-log and stationary phases was also confirmed within these cultures. This shows that *C. reinhardtii* can achieve normal growth under reduced N consumption rates for both KNO_3 and NH_4Cl conditions. This contributes to the idea that *C. reinhardtii*'s growth between the mid-log phase and stationary phase is due to a metabolic switch from N uptake to possible internal N use.

3.3 – Urea as an N source

Urea gets converted to ammonia through the formula:

$CO(NH_2)_2 + H_2O \rightarrow 2\ NH_3 + CO$ (Duo et al., 1992).

We expected to see a similar growth pattern to that of NH_4Cl at twice the concentration. *C. reinhardtii* WT strains grown in 4.0 mM and 2.0 mM urea medium presented similar growth patterns and biomass values, as seen in Figure 8 and Table 6. This shows that *C. reinhardtii* is capable of maximum growth under 2.0 mM urea, which is equivalent to 4.0 mM NH_4Cl. With the one-way ANOVA, 8.0 mM and 4.0 mM NH_4Cl culture evaluation values (Table 3 and either Table 1 or 2) are compared against 4.0 mM

and 2.0 mM urea conditions culture evaluation values at the stationary phase (Tables 6-7). This test showed that there were no significant differences between the growth rate (p-value = 0.31; F-stat. 1.8 < F-crit. 18.5) and growth maximum (p-value = 0.183; F-stat. 4.0 < F-crit. 18.5). This suggests that *C. reinhardtii* have similar growth patterns between 8.0 – 4.0 mM NH_4Cl and 4.0 – 2.0 mM urea as expected. Interestingly, amongst three of my urea photobioreactor experiments with their replicates, 1.0 mM urea cultures seem to produce lower growth maximum values compared to 0.5 mM urea cultures (Fig. 8), which does not line up with growth patterns shown in 2.0 mM and 1.0 mM NH_4Cl (Fig. 1 and 2). A growth pattern they do share is that the lowest N provision culture, 0.5 mM, in urea and NH_4Cl produce the largest doubling time compared to 1.0 mM. This can also be seen with KNO_3 cultures. However, their biomass growth remained lower in the higher-concentration cultures. This may be possible due to cultures responding to the immediate N-limited environment within their environment by reducing the consumption rate and switching to metabolizing internal N, a characteristic resembling N-salvaging response.

To determine whether consumption rates of urea would be like that of NH_4Cl cultures, quantification of urea remaining in the medium was also performed. Using the standard curves in Figure 9A-B, urea concentration was quantified, and the data obtained is in Table 7. Figure 9A standard curve was used for 4.0 – 1.0 mM urea culture samples and Figure 9B standard curve was for 1.0 – 0.5 mM samples. By the stationary phase, urea cultures grown in 2.0 – 0.5 mM have nearly depleted the available N in the medium, like the NH_4Cl cultures. However, 4.0 mM urea cultures still had a reserve of 1.01 ± 0.34 mM urea within the medium by the stationary phase, whereas the 8.0 mM NH_4Cl cultures were able to use up most of their N. With the cell density measures in Figure 10 and

Table 7, 4.0 – 2.0 mM urea cultures had the highest difference in cell density growth between the mid-log phase and stationary phase compared to the 1.0 – 0.5 mM cultures. Interestingly, at the stationary phase, 0.5 mM cultures had higher biomass OD values, even with near-depleted N in the medium (0.006 ± 0.01) compared to the 1.0 mM cultures. This could be due to the N-salvaging response prioritizing the degradation of protein contents that are not useful anymore, such as the urea amidolyase complex and its subunits, before the degradation of chloroplast (Schmollinger et al., 2014; Saroussi et al., 2017; West, 2023.

4 – Discussion

N availability is a key factor influencing the growth and physiological responses of *C. reinhardtii*. The present study investigated the effects of different nitrogen sources, NH_4Cl, KNO_3, and urea, on the growth dynamics of two WT strains, CC5370 and CC5119. Through the photobioreactor experiments, biomass productivity measurements, such as growth OD, growth rate, and doubling time, provided insights into how the N-sensing program integrates into observed N-use strategies. My results suggest two key findings. First, there is a regulatory mechanism where *C. reinhardtii* reduces the rate of N consumption upon experiencing extreme nitrogen stress, likely as an adaptive strategy to sustain survival under prolonged nitrogen limitation (Schmollinger et al., 2014; Park et al., 2015). This can be seen commonly across all three N conditions (NH_4Cl, KNO_3, and urea) that were tested in my study. Cultures that had fewer N provisions had consumed the majority of N within the medium by the mid-log phase, continued to grow to their maximum biomass and cell divide to the stationary phase.

Secondly, under reduced N consumption, *C. reinhardtii* also begins to shift its metabolic priorities from N uptake and assimilation into internal N metabolism, which was observed in the stationary phase with nearly consumed N medium, yet maximum growth was maintained many hours after reaching this phase. This may be possible due to cultures' response to the immediate N-limited environment within their environment by reducing the consumption rate, preventing complete N starvation and switching to metabolizing internal N, a characteristic described as N-salvaging in (Schmollinger et al., 2014; Saroussi et al., 2017; West, 2023). This N-regulation mechanism could also provide insight into the cell cycle of *C. reinhardtii,* which has a temporal separation of

photosynthetic cell growth and rapid cell division (Cross and Umen, 2015). Under N-salvaging, photosynthetic cell growth is halted possibly due to N, as a key component of chlorophyll, no longer being available for this activity. Hence, cell division could continue to occur, as we can see with my cell density graphs in Figures 4, 7 and 10.

Interestingly, I observed a phenomenon in 1.0 mM urea cultures, which exhibited lower growth maximum values than in 0.5 mM urea cultures. This deviation may indicate a response where *C. reinhardtii* reveals its N-salvaging strategy under immediate nitrogen limitation to favour the degradation of proteins that are no longer useful such as the urea amidolyase complex that *C. reinhardtii* uses for urea conversion (Park et al., 2015; Liang et al., 2024). To confirm whether this is the case, a follow-up study could be performed that allows urea cultures to grow to the stationary phase until the death phase at which biomass OD values drop and attempt to rescue maximum growth through the provision of more urea. If urea contents remain high within the medium, it could suggest that proteins necessary for urea assimilation are one of the priorities for N salvaging. Additionally, this experiment can be done with the other N sources: NH_4Cl and KNO_3 to identify which protein contents for which N assimilation pathway are degraded first. This could also further elucidate which N sources are preferred by photosynthetic eukaryotes if that assimilation pathway is least affected by N-salvaging.

There were limitations to my study, which included the time constraints for the scope of this study. For efficiency, I merged the two WT strains as replicates for the KNO_3, and urea experiments to assess normal growth physiological responses. This can be adjusted by running similar experiments once more to obtain true triplicates of each WT strain and analyze their responses separately to truly show their biological functions.

Having two WT strains analyzed separately and showing similar functions can help identify that these functions can occur in nature. Additionally, I had modified my quantification methods for NH_4Cl and urea from using the Hanna Instruments Multiparameter Photometer to using the BioTek Synergy H1 Microplate Reader. As my urea quantification protocol involves the use of urease to convert it into NH_4^+, both quantification methods should have been similar in measuring NH_4^+ in the medium. However, due to the lack of Nessler reagent availability remaining in the lab, I had to modify my protocol to work with the remaining reagents. If this study were to be done once more, I would adapt to using the microplate reader instrument for efficient absorbance measurements and less reagent use.

Altogether, these findings support the hypothesis that N-sensing mechanisms regulate N uptake and utilization for optimal growth under varying N availability through distinct uptake and consumption patterns among different nitrogen sources. Future studies should explore the molecular basis of N storage and regulation in *C. reinhardtii*, to further investigate temporal cues that allow this alga to switch between uptake and cell division behaviours. Additionally, with my current data, further analyses of the growth rate data present a growth activity curve to distinctly show the conversion of the N sources into biomass production. Doing so can further elucidate the temporal points at which N metabolism is regulated and switch from N scavenging to N salvaging. By leveraging the internal biological regulatory mechanisms of photosynthetic eukaryotes, sustainable agricultural practices can be refined to support food production in an era of climate change and resource limitations.

Literature Cited

Bellido-Pedraza, C.M., Calatrava, V., Sanz-Luque, E., Tejada-Jiménez, M., Llamas, Á., Plouviez, M., Guieysse, B., Fernández, E., and Galván, A. 2020. Chlamydomonas reinhardtii, an Algal Model in the Nitrogen Cycle. Plants (Basel), **9**: 903. https://doi.org/10.3390/plants9070903.

Cawse, P.A. (1967). The determination of nitrate in soil solutions by ultraviolet spectrophotometry. Analyst, **92**: 311–315. https://doi.org/10.1039/AN9679200311.

Chaney, A.L., and Marbach, E.P. 1962. Modified Reagents for Determination of Urea and Ammonia. Clinical Chemistry, **8**: 130–132. https://doi.org/10.1093/clinchem/8.2.130.

Cross, F.R., and Umen, J.G. 2015. The Chlamydomonas cell cycle. Plant Journal **82**(3): 370–392. doi:10.1111/tpj.12795.

Duo, W., Dam-Johansen, K., and Østergaard, K. 1992. Kinetics of the gas-phase reaction between nitric oxide, ammonia and oxygen. The Canadian Journal of Chemical Engineering, **70**: 1014–1020. https://doi.org/10.1002/cjce.5450700525.

D19 Committee. 2021. Standard Test Methods for Ammonia Nitrogen In Water. ASTM Manual
Of Water and Environmental Technology, D1426. https://doi.org/10.1520/D142615R21E01.

Fan, X., Naz, M., Fan, X., Xuan, W., Miller, A.J., and Xu, G. 2017. Plant nitrate transporters: from gene function to application. Journal of Experimental Botany, **68**: 2463–2475.

Fernandez, E., and Galvan, A. 2007. Inorganic nitrogen assimilation in Chlamydomonas. Journal of Experimental Botany, **58**: 2279–2287.

Firbank, L.G. 2005. Striking a new balance between agricultural production and biodiversity. Annals of Applied Biology, **146**: 163–175. https://doi.org/10.1111/j.1744-7348.2005.040078.x.

Fukase, E., and Martin, W. 2020. Economic growth, convergence, and world food demand and supply. World Development, **132**: 104954.

Glibert, P.M., Wilkerson, F.P., Dugdale, R.C., Raven, J.A., Dupont, C.L., Leavitt, P.R., Parker, A.E., Burkholder, J.M., and Kana, T.M. 2016. Pluses and minuses of ammonium and nitrate uptake and assimilation by phytoplankton and implications for productivity and community composition, with emphasis on nitrogen-enriched conditions. Limnology and Oceanography, **61**: 165–197. https://doi.org/10.1002/lno.10203.

Giordano, M., and Raven, J. A. 2014. Nitrogen and sulfur assimilation in plants and algae.Aquat. Bot., **118**: 45–61. doi: 10.1016/j.aquabot.2014.06.012

Gorman, D.S., and Levine, R.P. 1965. Cytochrome f and plastocyanin: their sequence in the photosynthetic electron transport chain of Chlamydomonas reinhardi. Proc Natl Acad Sci USA, **54**: 1665–1669. https://doi.org/10.1073/pnas.54.6.1665.

Griffiths, G., Burke, B., and Lucocq, J. 1993. Fine structure immunocytochemistry. Springer-Verlag, Berlin.

Hachiya, T., and Sakakibara, H. 2016 Interactions between nitrate and ammonium in their uptake, allocation, assimilation, and signaling in plants. Journal of Experimental Botany, **68**: 2501–2512.

Harris, E.H. 2009. The *Chlamydomonas* sourcebook: introduction to *Chlamydomonas* and its laboratory use, 2nd edn. Academic Press, Oxford, United Kingdom.

Hirel, B., Tétu, T., Lea, P.J., and Dubois, F. (2011). Improving Nitrogen Use Efficiency in Crops for Sustainable Agriculture. Sustainability, **3**: 1452–1485. https://doi.org/10.3390/su3091452.

Jia, M., Munz, J., Lee, J., Shelley, N., Xiong, Y., Joo, S., Jin, E.S., and Lee, J.H. 2022. The bHLH family NITROGEN-REPLETION INSENSITIVE1 represses nitrogen starvation-induced responses in *Chlamydomonas reinhardtii*. The Plant Journal, **110**: 337–57.

Kant, S., Bi, Y.-M., and Rothstein, S.J. 2011. Understanding plant response to nitrogen limitation for the improvement of crop nitrogen use efficiency. J Exp Bot, **62**: 1499–1509. https://doi.org/10.1093/jxb/erq297.

Kawahara, J., Ishikawa, K., Uchimaru, T., and Takaya, H. 1997. Chemical Cross-Linking by Glutaraldehyde between Amino Groups: Its Mechanism and Effects. *In* Polymer Modification. *Edited by* G. Swift, C.E. Carraher, and C.N. Bowman. Springer US, Boston, MA. pp. 119–131.

Kou, Z., Bei, S., Sun, J., and Pan, J. 2013. Fluorescent measurement of lipid content in the model organism *Chlamydomonas reinhardtii*. Journal of Applied Phycology, **25**: 1633–1641.

Krajewska, B., and Zaborska, W. 1999. The effect of phosphate buffer in the range of pH 5.80–8.07 on jack bean urease activity. Journal of Molecular Catalysis B: Enzymatic, **6**: 75–81. https://doi.org/10.1016/S1381-1177(98)00129-5.

Li, H., Hu, B., and Chu, C. 2017. Nitrogen use efficiency in crops: Lessons from *Arabidopsis* and rice. Journal of Experimental Botany, **68**: 2477–2488.

Liang, H., Lin, S., Chen, Y., Wang, J., Aslam, M., Chen, J., Du, H., and Li, T. 2024. Urea amidolyase as the enzyme for urea utilization in algae: functional display in Chlamydomonas reinhardtii and evolution in algae. Preprint at bioRxiv, https://doi.org/10.1101/2024.05.16.594469 https://doi.org/10.1101/2024.05.16.594469.

Liu, Y., and von Wirén, N. 2017. Ammonium as a signal for physiological and morphological responses in plants. Journal of Experimental Botany, **68**: 2581–2592. https://doi.org/10.1093/jxb/erx086.

Loqué, D., and von Wirén, N. 2004. Regulatory levels for the transport of ammonium in plant roots. Journal of Experimental Botany, **55**: 1293–1305.

Lim, J., Fernández, C.A., Lee, S.W., and Hatzell, M.C. 2021. Ammonia and Nitric Acid Demands for Fertilizer Use in 2050. ACS Energy Letters, **6**: 3676–3685.

Magasanik, B., and Kaiser, C.A. 2002. Nitrogen regulation in *Saccharomyces cerevisiae*. Gene, **290**: 1–18.

Moore, D. S., Notz, W. I, & Flinger, M. A. 2013. The basic practice of statistics (6th ed.). New York, NY: W. H. Freeman and Company

Munz, J., Xiong, Y., Kim, J.Y.H., Sung, Y.J., Seo, S., Hong, R.H., Kariyawasam, T., Shelley, N., Lee, J., Sim, S.J., Jin, E., and Lee, J.-H. 2020. Arginine-fed cultures

generates triacylglycerol by triggering nitrogen starvation responses during robust growth in *Chlamydomonas*. Algal Research, **46**: 101782.

Ota, R., Ohkubo, Y., Yamashita, Y., Ogawa-Ohnishi, M., and Matsubayashi, Y. 2020. Shoot-to-root mobile CEPD-like 2 integrates shoot nitrogen status to systemically regulate nitrate uptake in Arabidopsis. Nat. Commun., **11**: 641. https://doi.org/10.1038/s41467-020-14440-8.

Park, J.-J., Wang, H., Gargouri, M., Deshpande, R.R., Skepper, J.N., Holguin, F.O., Juergens, M.T., Shachar-Hill, Y., Hicks, L.M., and Gang, D.R. 2015. The response of Chlamydomonas reinhardtii to nitrogen deprivation: a systems biology analysis. The Plant Journal, **81**: 611–624. https://doi.org/10.1111/tpj.12747.

Rani, V., Shetty, P., and Maróti, G. 2024. Comparative transcriptome study highlights the versatility of nitrogen metabolism in *Chlamydomonas*. Algal Research, **79**: 103458.

Salomé, P.A., and Merchant, S.S. 2019. A Series of Fortunate Events: Introducing Chlamydomonas as a Reference Organism. Plant Cell, **31**: 1682–1707. https://doi.org/10.1105/tpc.18.00952.

Sanz-Luque, E., Chamizo-Ampudia, A., Llamas, A., Galvan, A., and Fernandez, E. 2015. Understanding nitrate assimilation and its regulation in microalgae. Front. Plant Sci. **6**: 899. https://doi.org/10.3389/fpls.2015.00899.

Saroussi, S., Sanz-Luque, E., Kim, R.G., and Grossman, A.R. 2017. Nutrient scavenging and energy management: acclimation responses in nitrogen and sulfur deprived *Chlamydomonas*. Current Opinion in Plant Biology, **39**: 114–122.

Schmollinger, S., Muhlhaus, T., Boyle, N.R., Blaby, I.K., Casero, D., Mettler, T., Moseley, J.L., Kropat, J., Sommer, F., Strenkert, D., Hemme, D., Pellegrini, M., Grossman, A.R., Stitt, M., Schroda, M., and Merchant, S.S. 2014. Nitrogen-sparing mechanisms in *Chlamydomonas* affect the transcriptome, the proteome, and photosynthetic metabolism. Plant Cell, **26**: 1410–1435.

Tilman, D., Fargione, J., Wolff, B., D'Antonio, C., Dobson, A., Howarth, R., Schindler, D., Schlesinger, W.H., Simberloff, D., and Swackhamer, D. 2001. Forecasting Agriculturally Driven Global Environmental Change. Science, **292**: 281–284. https://doi.org/10.1126/science.1057544.

Tilman, D., Cassman, K.G., Matson, P.A., Naylor, R., and Polasky, S. 2002. Agricultural sustainability and intensive production practices. Nature, **418**: 671–677. https://doi.org/10.1038/nature01014.

Tuttle, J.T., Williams, J.R., and Higgs, D.C. 2020. Characterization of a *Chlamydomonas reinhardtii* mutant strain with tolerance to low nitrogen and increased growth and biomass under nitrogen stress. Algal Research, **50**: 102000. https://doi.org/10.1016/j.algal.2020.102000.

United Nations. 2019. World Population Prospects: The 2019 Revision. New York: United Nations.

Wang, W.H., Köhler, B., Cao, F.Q., Liu, G.W., Gong, Y.Y., Song, S., Song, Q.C., Cheng, X.Y., Garnett, T., Okamoto, M., Qin, R., Mueller-Roeber, B., Tester, M., and Liu, L.H. 2012. Rice DUR3 mediates high affinity urea transport and plays an effective role in improvement of urea acquisition and utilization when expressed in *Arabidopsis*. New Phytologist, **193**: 432–444.

Wang, Y.Y., Hsu, P.K., and Tsay, Y.F. 2012. Uptake, allocation and signaling of nitrate. Trends in Plant Science, **17**: 458–467.

West, T.P. 2023. Pyrimidine Biosynthesis and Ribonucleoside Metabolism in Species of *Pseudomonas*. Fermentation, **9**: 955.

Xu, G., Fan, X., and Miller, A.J. (2012). Plant nitrogen assimilation and use efficiency. Annu Rev Plant Biol, **63**: 153–182. https://doi.org/10.1146/annurev-arplant-042811-105532.

Zhang, Z., Tan, Y., Wang, W., Bai, W., Fan, J., Huang, J., Wan, M., and Li, Y. 2019. Efficient heterotrophic cultivation of *Chlamydomonas reinhardtii*. Journal of Applied Phycology, **31**: 1545–1554.

Figures and Tables

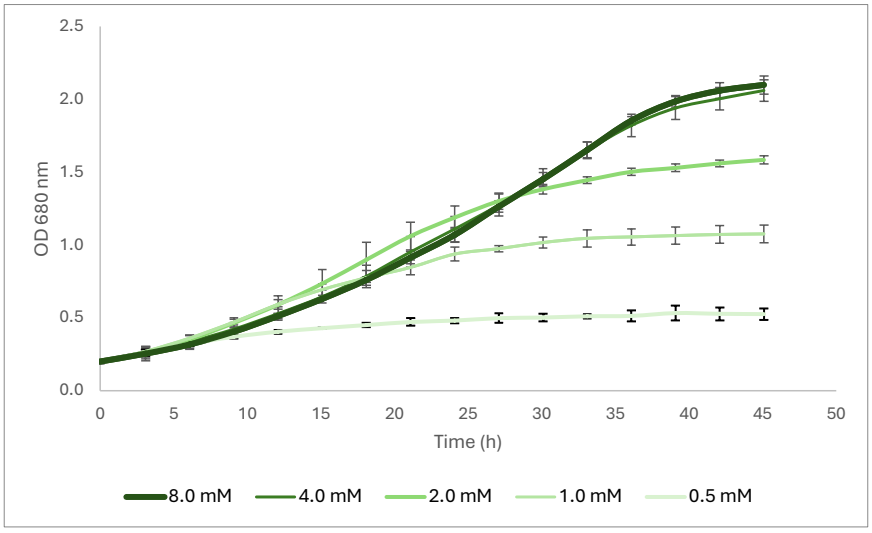

Figure 1. Triplicate log2-fold average growth of CC5370 in NH4Cl-TAP at 8.0 – 0.5 mM.

Error bars show SD.

Commented [JD1]: See comment in the list of figures re: same titles.

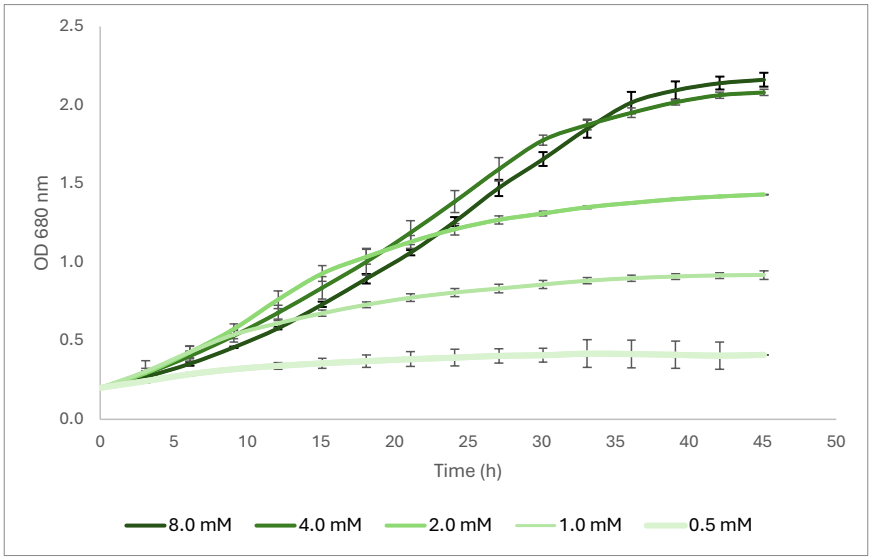

Figure 2. Mean and standard deviation growth of CC5119 in NH_4Cl-TAP at 8.0 – 0.5 mM.

A)

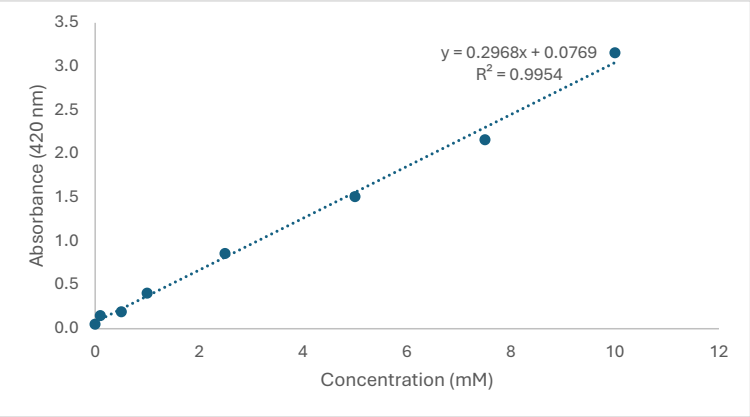

B)

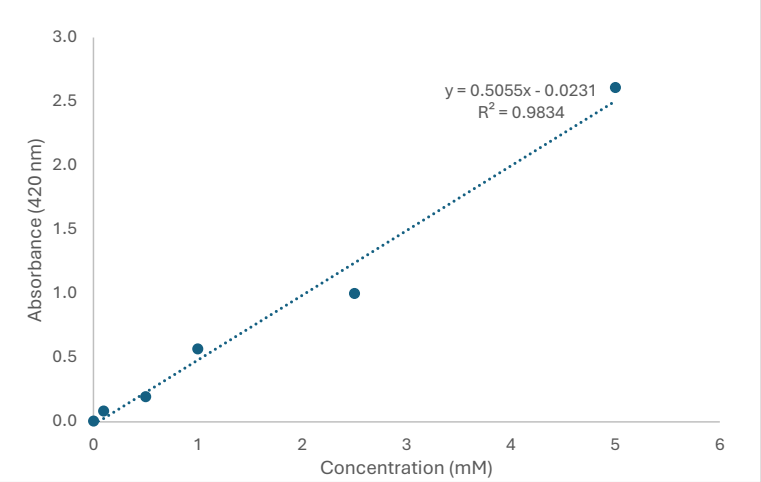

Figure 3. Standard Curve for 1.0 mL NH_4Cl samples. A) Used to quantify samples for NH_4Cl cultures from 4.0 mM and below. B) Standard curve for 0.5 mL NH_4Cl samples to quantify 8.0 mM NH_4Cl cultures.

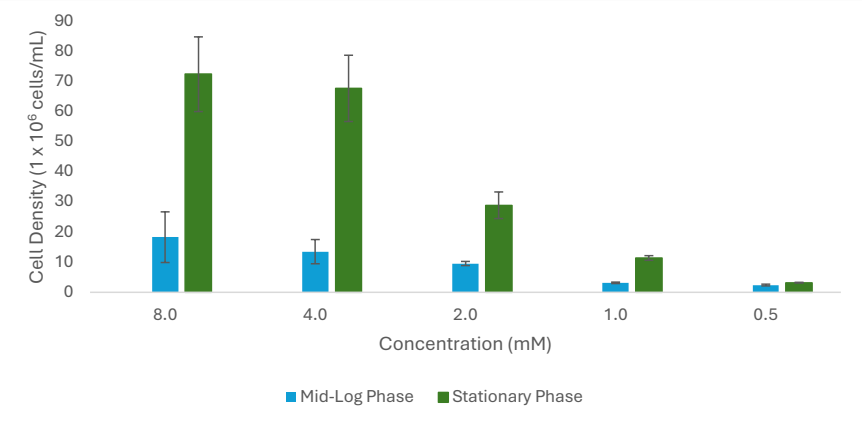

Figure 4. Mean and standard deviation of wild-type strains cell density (cells/mL) in 8.0 – 0.5 mM NH_4Cl-TAP using data from Table 3.

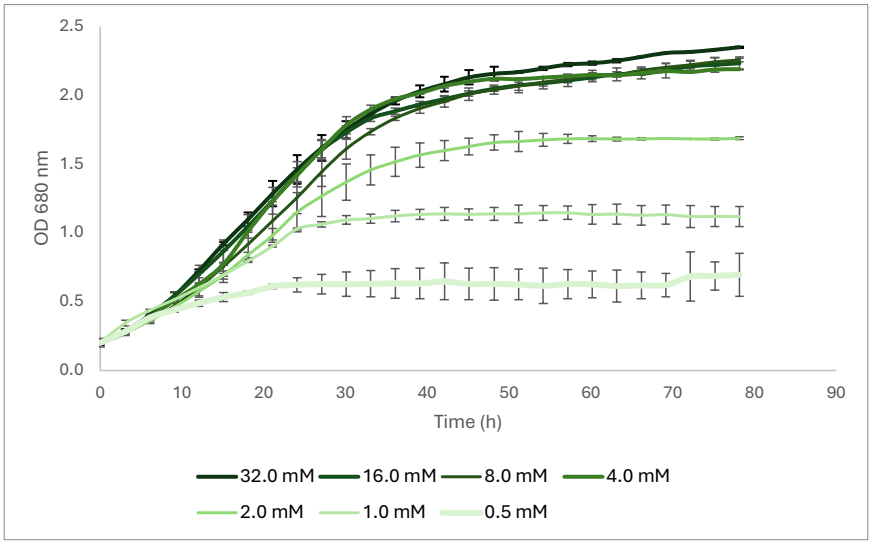

Figure 5. Mean and standard deviation of wild-type strains in KNO_3-TAP at 32.0 – 0.5 mM.

A)

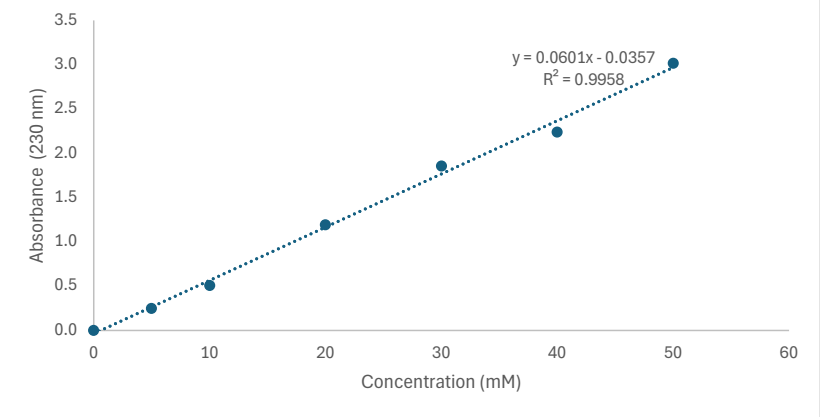
y = 0.0601x - 0.0357
R² = 0.9958
Absorbance (230 nm)
Concentration (mM)
0.0
0.5
1.0
1.5
2.0
2.5
3.0
3.5
0
10
20
30
40
50
60

B)

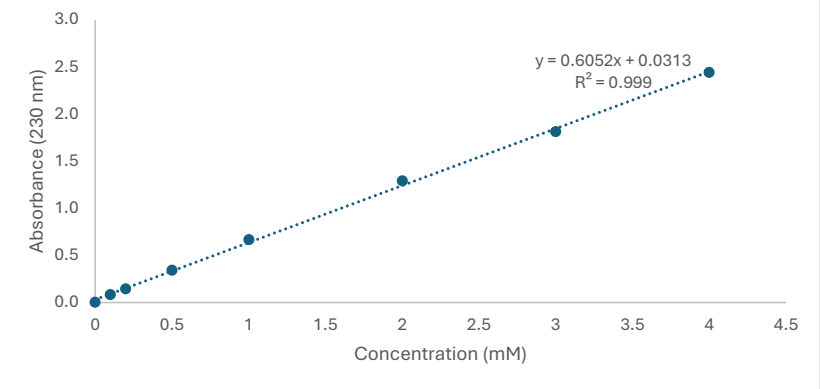
y = 0.6052x + 0.0313
R² = 0.999
Absorbance (230 nm)
Concentration (mM)
0.0
0.5
1.0
1.5
2.0
2.5
3.0
0
0.5
1
1.5
2
2.5
3
3.5
4
4.5

C)

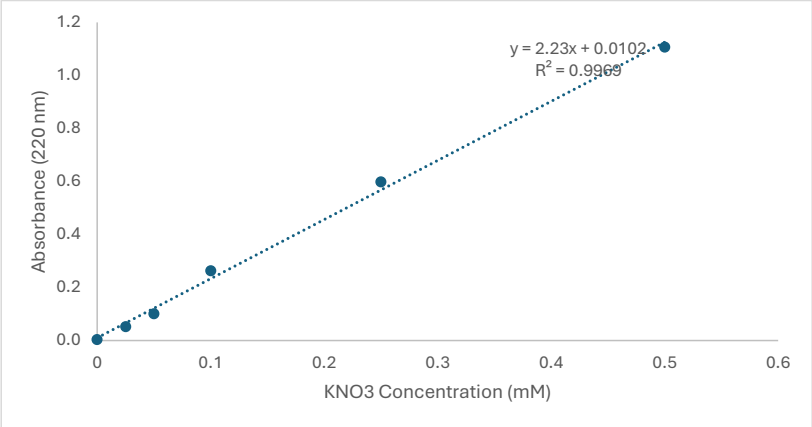

Figure 6. Standard curves to quantify remaining KNO_3 in culture samples. A) For 32.0 – 4.0 mM KNO_3 samples. B) For 4.0 – 1.0 mM KNO_3 samples. C) For 1.0 - 0.5 mM KNO_3 samples.

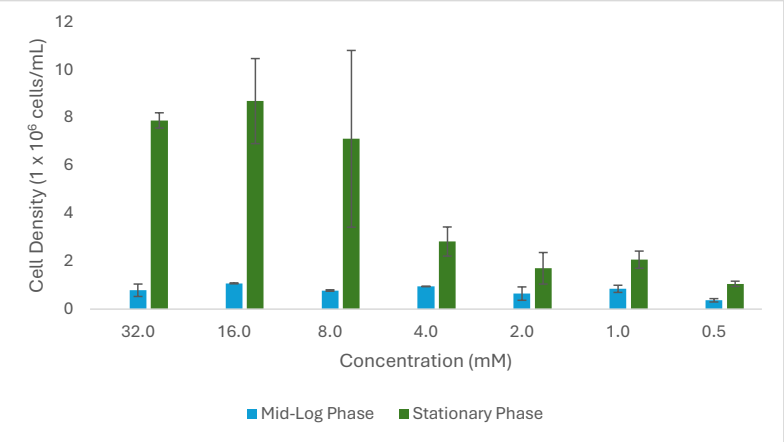

Figure 7. Mean and standard deviation of wild-type strains cell density (cells/mL) in 32.0 – 0.5 mM KNO_3-TAP using data from Table 5.

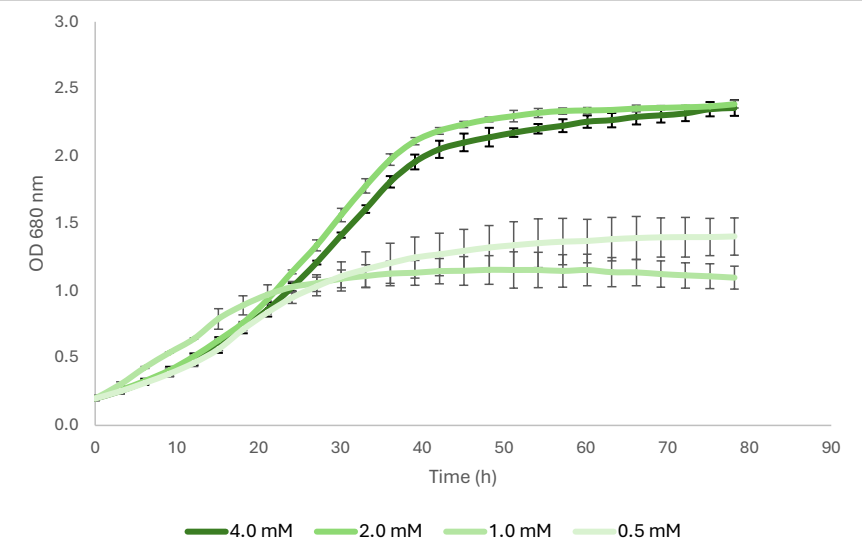

Figure 8. Mean and standard deviation of wild-type strains in Urea-TAP in 4.0 – 0.5 mM.

A)

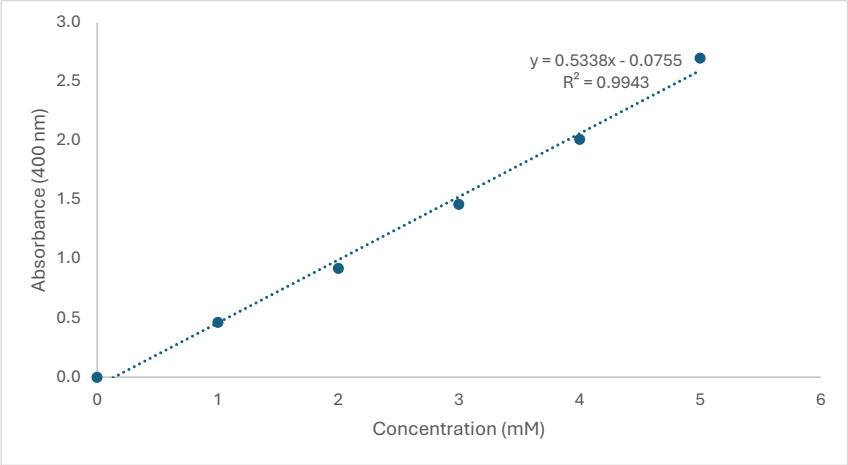

B)

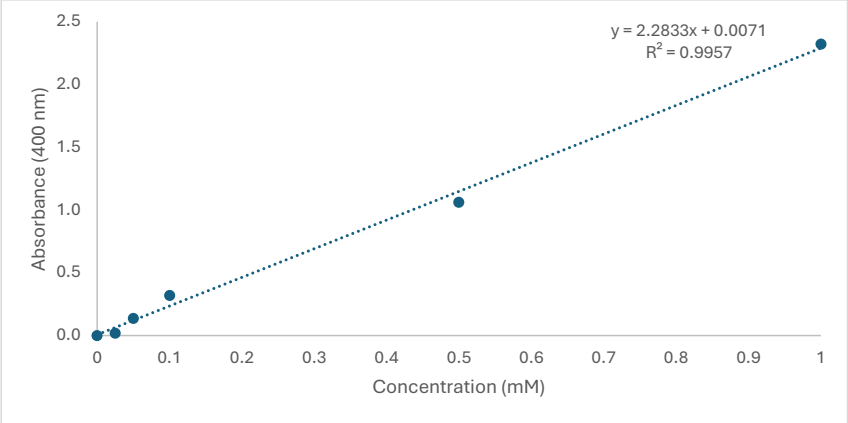

Figure 9. Standard curve for quantifying urea concentrations within Urea-TAP grown cultures A) For urea cultures from 4.0 – 1.0 mM. B) For urea cultures from 1.0 – 0.5 mM.

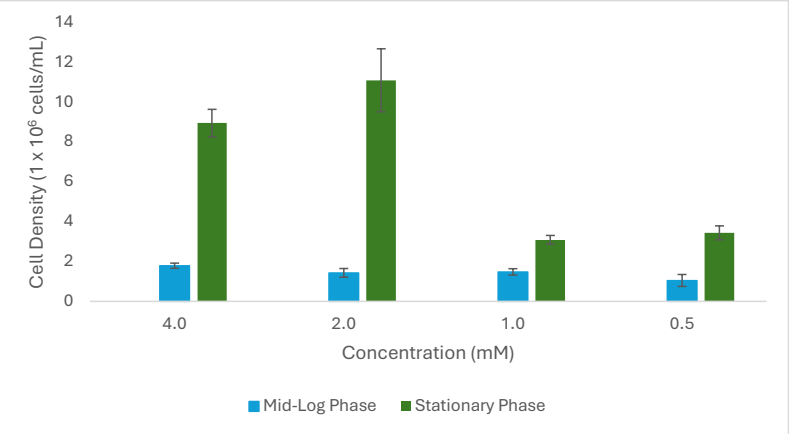

Figure 10. Mean and SD cell concentrations (cells/mL) of WT strains in 4.0 – 0.5 mM Urea-TAP. Cell density measures are scaled down from 1 x 10^6 cells/mL.

Table 1. Triplicate mean and standard deviation of growth maximum, growth rate and doubling time of CC5370 cultures grown in 8.0 – 0.5 mM NH_4Cl-TAP range.

Concentrations (mM)	Avg Growth Rate (μ) [OD]	Avg Doubling Time (td) [h]
8.0	0.024 ± 0.001	29.1 ± 1.09
4.0	0.026 ± 0.001	26.7 ± 1.23
2.0	0.030 ± 0.002	23.0 ± 1.34
1.0	0.032 ± 0.001	21.9 ± 0.41
0.5	0.018 ± 0.000	54.9 ± 0.81

Table 2. Triplicate mean and standard deviation of growth maximum, growth rate and doubling time of CC5119 cultures grown in 8.0 – 0.5 mM NH_4Cl-TAP range.

Concentrations (mM)	Avg Growth Rate (μ) [OD]	Avg Doubling Time (td) [h]
8.0	0.030 ± 0.000	23.2 ± 0.25
4.0	0.038 ± 0.002	18.3 ± 0.80
2.0	0.043 ± 0.001	16.1 ± 0.54
1.0	0.037 ± 0.001	19.0 ± 0.63
0.5	0.013 ± 0.000	54.9 ± 1.32

Table 3. Wild-type strain culture evaluations at each critical growth phase. Medium concentrations at each tested NH_4Cl condition were obtained using standard curves from Figure 3. Values are presented as means with standard deviation. Cell density measures are scaled down from 1 x 10^6 cells/mL.

Lag Phase			
NH_4Cl Concentration	Quantified Concentration (mM)	Growth OD (680 nm)	Cell Density (cells/mL)
8.0	8.21 ± 0.034	0.00	0.00
4.0	4.36 ± 0.032	0.00	0.00
2.0	2.34 ± 0.046	0.00	0.00
1.0	1.40 ± 0.031	0.00	0.00
0.5	0.553 ± 0.017	0.00	0.00
Mid-Log Phase			
NH_4Cl Concentration	Quantified Concentration (mM)	Growth OD (680 nm)	Cell Density (cells/mL)
8.0	3.00 ± 0.059	1.07 ± 0.058	18.3 ± 8.41
4.0	0.329 ± 0.005	1.11 ± 0.045	13.5 ± 4.02
2.0	0.263 ± 0.007	0.915 ± 0.029	9.56 ± 0.69
1.0	0.240 ± 0.024	0.654 ± 0.016	3.15 ± 0.24
0.5	0.156 ± 0.034	0.359 ± 0.036	2.42 ± 0.29
Stationary Phase			
NH_4Cl Concentration	Quantified Concentration (mM)	Growth OD (680 nm)	Cell Density (cells/mL)
8.0	0.156 ± 0.012	2.174 ± 0.075	72.4 ± 12.4
4.0	0.134 ± 0.013	2.176 ± 0.068	67.7 ± 11.0
2.0	0.151 ± 0.012	1.642 ± 0.027	28.9 ± 4.42
1.0	0.143 ± 0.017	1.081 ± 0.026	11.4 ± 0.77
0.5	0.110 ± 0.018	0.528 ± 0.030	3.21 ± 0.11

Table 4. Triplicate mean and standard deviation growth rate and doubling time of wild-type strains grown in 32.0 – 0.5 mM KNO_3-TAP range.

Concentrations (mM)	Avg Growth Rate (μ) [OD]	Avg Doubling Time (td) [h]
32.0	0.040 ± 0.002	17.2 ± 0.83
16.0	0.039 ± 0.002	17.6 ± 0.67
8.0	0.031 ± 0.001	22.2 ± 0.97
4.0	0.035 ± 0.001	19.8 ± 0.28
2.0	0.031 ± 0.001	22.7 ± 0.93
1.0	0.034 ± 0.001	20.5 ± 0.62
0.5	0.026 ± 0.001	27.0 ± 0.91

Table 5. Wild-type strain culture evaluations at each critical growth phase. Medium concentrations at each tested KNO_3-TAP condition were obtained using standard curves from Figure 6. Values are presented as means with standard deviation. Cell density measures are scaled down from 1 x 10^6 cells/mL.

Lag Phase			
KNO_3 Concentration	Quantified Concentration (mM)	Growth OD (680 nm)	Cell Density (cells/mL)
32.0	32.4 ± 0.76	0.00	0.00
16.0	17.0 ± 0.26	0.00	0.00
8.0	7.73 ± 0.11	0.00	0.00
4.0	3.60 ± 0.05	0.00	0.00
2.0	2.16 ± 0.05	0.00	0.00
1.0	1.16 ± 0.004	0.00	0.00
0.5	0.57 ± 0.01	0.00	0.00
Mid-Log Phase			
KNO_3 Concentration	Quantified Concentration (mM)	Growth OD (680 nm)	Cell Density (cells/mL)
32.0	28.0 ± 0.20	1.30 ± 0.31	0.98 ± 0.4
16.0	13.8 ± 1.17	1.18 ± 0.35	0.67 ± 0.1
8.0	5.00 ± 1.50	1.16 ± 0.41	1.07 ± 0.01
4.0	2.56 ± 0.54	0.865 ± 0.04	0.89 ± 0.18
2.0	1.27 ± 0.07	0.996 ± 0.07	0.89 ± 0.12
1.0	0.128 ± 0.01	0.628 ± 0.004	0.85 ± 0.15
0.5	0.022 ± 0.01	0.437 ± 0.10	0.37 ± 0.07
Stationary Phase			
KNO_3 Concentration	Quantified Concentration (mM)	Growth OD (680 nm)	Cell Density (cells/mL)
32.0	26.1 ± 0.49	2.55 ± 0.20	8.19 ± 0.26
16.0	9.60 ± 0.68	2.41 ± 0.06	8.37 ± 0.82
8.0	3.87 ± 0.32	2.46 ± 0.05	8.03 ± 1.48
4.0	0.208 ± 0.03	2.34 ± 0.04	9.45 ± 0.68
2.0	0.17 ± 0.11	1.68 ± 0.03	3.09 ± 0.20
1.0	0.044 ± 0.02	1.01 ± 0.10	2.07 ± 0.36
0.5	0.021 ± 0.03	0.516 ± 0.10	1.06 ± 0.11

Table 6. Triplicate mean and standard deviation growth rate and doubling time of wild-type strains grown in 4.0 – 0.5 mM Urea-TAP range.

Concentrations (mM)	Avg Growth Rate (μ) [OD]	Avg Doubling Time (td) [h]
4.0	0.023 ± 0.001	30.1 ± 1.6
2.0	0.024 ± 0.001	28.9 ± 0.7
1.0	0.038 ± 0.001	18.3 ± 0.5
0.5	0.021 ± 0.001	32.4 ± 0.9

Table 7. Wild-type strain culture evaluations at each critical growth phase. Medium concentrations at each tested Urea-TAP condition were obtained using standard curves from Figure 9. Values are presented as means with standard deviation. Cell density measures are scaled down from 1 x 10^6 cells/mL.

Lag Phase			
Urea Concentration (mM)	Quantified Concentration (mM)	Growth OD (680 nm)	Cell Density (cells/mL)
4.0	4.19 ± 0.39	0	0
2.0	2.65 ± 0.65	0	0
1.0	1.00 ± 0.16	0	0
0.5	0.54 ± 0.07	0	0
Mid-Log Phase			
Urea Concentration (mM)	Quantified Concentration (mM)	Growth OD (680 nm)	Cell Density (cells/mL)
4.0	1.86 ± 0.58	1.17 ± 0.04	1.79 ± 0.13
2.0	1.29 ± 0.18	1.09 ± 0.05	1.43 ± 0.22
1.0	0.69 ± 0.30	0.55 ± 0.11	1.48 ± 0.16
0.5	0.17 ± 0.03	0.45 ± 0.12	1.05 ± 0.30
Stationary Phase			
Urea Concentration (mM)	Quantified Concentration (mM)	Growth OD (680 nm)	Cell Density (cells/mL)
4.0	1.01 ± 0.34	2.43 ± 0.18	8.95 ± 0.69
2.0	0.157 ± 0.01	2.38 ± 0.02	11.1 ± 1.58
1.0	0.051 ± 0.01	1.17 ± 0.13	3.09 ± 0.22
0.5	0.006 ± 0.01	1.32 ± 0.02	3.44 ± 0.35